ARID5B influences B-cell development and function in mouse

Charnise Goodings,[1*] Xujie Zhao,[1*] Shannon McKinney-Freeman,[2] Hui Zhang[3] and Jun J. Yang[1,4]

[1]Department of Pharmaceutical Sciences, St. Jude Children's Research Hospital, Memphis, TN, USA; [2]Department of Hematology, St. Jude Children's Research Hospital, Memphis, TN, USA; [3]Department of Hematology/Oncology, Shanghai Children's Medical Center, Shanghai, China and [4]Department of Oncology, St. Jude Children's Research Hospital, Memphis, TN, USA.

**CG and XZ contributed equally as co-first authors.*

Correspondence: J. J. Yang
jun.yang@stjude.org

Received: March 29, 2022.
Accepted: July 29, 2022.
Prepublished: August 4, 2022.

https://doi.org/10.3324/haematol.2022.281157

Abstract

There is growing evidence for an inherited basis of susceptibility to childhood acute lymphoblastic leukemia. Genome-wide association studies by us and others have identified non-coding acute lymphoblastic leukemia risk variants at the *ARID5B* gene locus, but the molecular mechanisms linking *ARID5B* to normal and malignant hematopoiesis remain largely unknown. Using a *Vav1*-driven transgenic mouse model, we characterized the role of *Arid5b* in hematopoiesis *in vivo*. *Arid5b* overexpression resulted in a dramatic reduction in the proportion of circulating B cells, immature, and mature B-cell fractions in the peripheral blood and the bone marrow, and also a decrease of follicular B cells in the spleen. There were significant defects in B-cell activation upon *Arid5b* overexpression *in vitro* with hyperactivation of B-cell receptor signaling at baseline. In addition, increased mitochondrial oxygen consumption rate of naïve or stimulated B cells of *Arid5b*-overexpressing mice was observed, compared to the rate of wild-type counterparts. Taken together, our results indicate that *ARID5B* may play an important role in B-cell development and function.

Introduction

Acute lymphoblastic leukemia (ALL) is the most common cancer in children, with an incidence peaking between 3 and 5 years of age.[1,2] Its early onset suggested a possible role of inherited genetic variations in susceptibility to ALL,[3] a possibility which is also supported by studies in monozygotic twins with concordant ALL.[4-6] Moreover, recent efforts by us and others in genome-wide association studies have provided unequivocal evidence for the genetic basis of ALL susceptibility, with more than 20 risk loci having been identified.[7-19] Among them, *ARID5B* consistently exhibits the strongest association signal across racial and ethnic groups,[9,12,16] with the risk variants specifically predisposing children to high-hyperdiploid ALL, in an age-related fashion. There is also emerging evidence that these non-coding variants can directly influence *ARID5B* transcription *in cis*.[20] By contrast, there has been a particular paucity of studies investigating the functions of *ARID5B* in hematopoiesis and how it influences B-cell biology.

ARID5B belongs to the AT rich interaction domain (ARID) protein family consisting of 15 members and characterized by a shared DNA-binding ARID domain.[21-24] Shortly after the identification of the *ARID5B* gene, its *in vivo* expression was characterized.[25] A broad biological function of *Arid5b* has been indicated by its wide expression in adult organs including lung, small intestine, kidney, muscle, heart, and brain. In the same study, consequences of silencing *Arid5b* were also investigated. Deficiency of *Arid5b* led to smaller body size and leanness at birth and reduced growth rate after birth. In the hematopoietic compartment, *Arid5b*$^{-/-}$ mice exhibited a range of transient defects in lymphocyte development, including reduction of cellularity in bone marrow, thymus, and spleen, and significant decreases in early T- and B-cell progenitors in the bone marrow of 3-week-old mice, while most of these abnormalities disappeared at 6 weeks old.[25] The leanness phenotype of the *Arid5b*$^{-/-}$ mouse was confirmed in another mouse model presenting with severely less brown adipose at birth, which could not be rescued by high-fat diets directly and is therefore implicated in adipogenesis.[26] The nuclear localization and superior binding affinity of ARID5B to the A/T-rich consensus sequence (AATA[C/T])[21,27] point to a potential function as a transcription factor. Indeed, by form-

ing a complex with PHF2, ARID5B can regulate glucose metabolism by activating the expression of *PEPCK* and *G6PC* in hepatocytes.[28] In natural killer (NK) cells, downregulation of *ARID5B* represses *UQCRB* expression and decreases mitochondrial membrane potential and mitochondrial oxidative metabolism, along with *BCL2* downregulation.[29] In T-ALL cells, the genome-wide binding profile of ARID5B-bound regions is strongly associated with active histone markers (H3K27ac and H3K4me3), pointing to ARID5B acting as a transcriptional activator.[30]

In this study, we established mouse models with overexpression and knockout of *Arid5b* in hematopoietic cells. Using these tools, we comprehensively evaluated the roles of *ARID5B* in hematopoiesis *in vivo*, especially B-cell development, providing new insights into its potential contribution to leukemia pathogenesis.

Methods

Arid5b mouse models

To establish the *Arid5b*-overexpression mouse model, we first knocked in the tetO cassette at the *Arid5b* locus. These mice were then crossed with *Vav1*-tTA animals (*Online Supplementary Figure S1A*) to induce *Arid5b* overexpression in hematopoietic cells (*Vav1*$^{+}$). Tail biopsies were submitted to Transnetyx (Cordova, TN, USA) for genotyping. Animal experiments were performed according to procedures approved by the St. Jude Children's Research Hospital Institutional Animal Care and Use Committee. Primers used for genotyping are detailed in *Online Supplementary Table S1*. Overexpression of *Arid5b* was confirmed by quantitative reverse transcriptase polymerase chain reaction in different hematopoietic cells. Primers used for the polymerase chain reaction are detailed in *Online Supplementary Table S2*.

Analysis of peripheral blood counts

Peripheral blood was collected from the retro-orbital plexus into capillary tubes and transferred into EDTA-coated tubes to prevent clotting. Blood samples were then submitted to St. Jude Veterinary Pathology Core for automated complete blood counting.

Flow cytometry

Peripheral blood was collected from the retro-orbital plexus of the mice. Bone marrow was isolated from dissected tibiae and femora. Spleens were surgically removed and homogenized into a cell suspension in Iscove modified Dulbecco medium. Cells were stained for surface markers followed by flow cytometry analysis using a BD LSR Fortessa (BD Biosciences, NJ, USA) and data were analyzed using FlowJo software (Tree Star, OR, USA). For cell cycle analysis, cells were fixed with the BD Cytofix/Cytoperm kit (BD Biosciences #554714) after cell surface staining followed by DAPI staining. Staining of apoptotic cells was done by cell surface staining, followed by labeling with annexin V (BD Biosciences #556420) and DAPI in annexin V staining buffer (BD Biosciences #556454). Representative flow cytometry plots are shown in *Online Supplementary Figures S2-S4*. Detailed information on the antibodies used is provided in *Online Supplementary Table S3*.

Colony-forming assay

Mouse bone marrow cells were plated in MethoCult M3434 or M3630 medium (StemCell Technologies #03434 and #03630, Vancouver, British Columbia, Canada) to characterize growth and differentiation of myeloid progenitors and pre-B-cell progenitors. Colonies were typed and enumerated by light microscopy after incubation for 7-10 days.

B-cell purification and activation

Splenic cell suspensions were prepared in magnetic-activated cell sorting (MACS) buffer (phosphate-buffered saline/2 mM EDTA/0.5% bovine serum albumin). CD43-negative resting B cells were isolated using the MACS B-cell isolation kit (Miltenyi Biotec, Bergisch Gladbach, Germany). Resting B cells were then activated either by lipopolysaccharide (LPS) from *Salmonella enterica* serotype typhimurium (Sigma-Aldrich #L6143, MO, USA) at 20 µg/mL or AffiniPure F(ab')$_2$ Fragment Goat Anti-Mouse IgM, µ Chain Specific (Jackson Immunoresearch Lab, PA, USA) at 10 µg/mL plus murine interleukin (IL)-4 (Peprotech # 214-14, NJ, USA) at 10 ng/mL at 400,000 cells/mL for 24 or 48 hours in RPMI 1640 (ThermoFisher #11875093), 1 × L-glutamine, 10% fetal bovine serum, 1 × essential amino acids, 1 × penicillin/streptomycin, 1 mM sodium pyruvate and 50 mM 2-mercaptoethanol.[31]

B-cell proliferation assay

For cell proliferation assays, the CellTiter 96 AQueous One Solution Cell Proliferation Assay system (Promega #G3852, WI, USA) was used according to the manufacturer's instructions. Two hundred thousand cells were placed into each well in a 96-well plate and 10 µL per well of CellTiter 96 AQueous One Solution reagent were added. After incubation for 1 hour in humidified 5% CO_2 atmosphere, absorbance at 490 nm was measured.

Results

Arid5b regulates hematopoiesis in mouse

Because *ARID5B* variants are linked to susceptibility to B-ALL, we suggest that this gene is involved in normal hematopoiesis, most likely B-lymphocyte development. To test this hypothesis, we generated a hematopoietic-specific *Arid5b* overexpression (*Arid5b*^{OE}) mouse model (*Online*

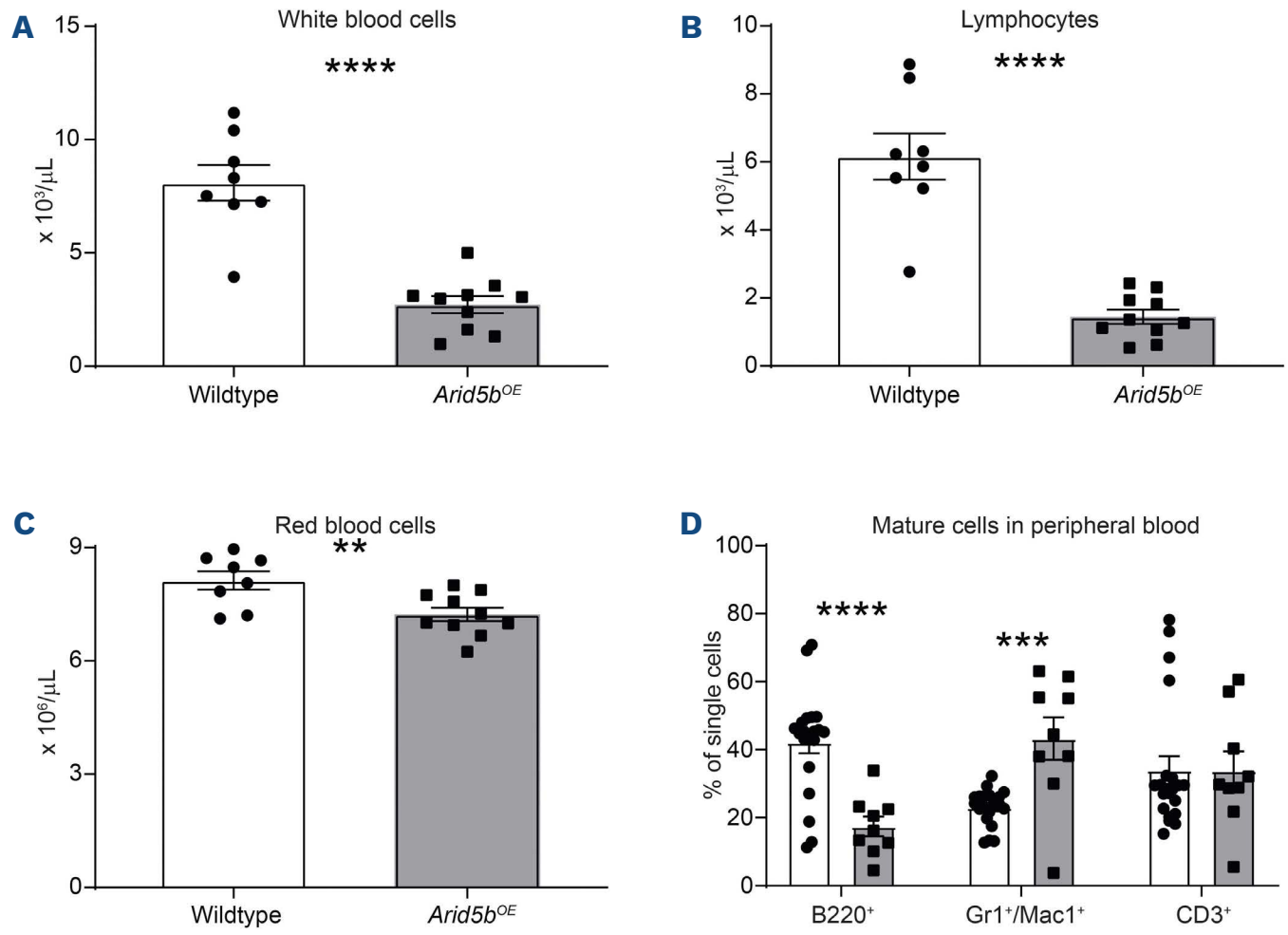

Figure 1. Effects of *Arid5b*^{OE} on hematopoietic cells in the peripheral blood. (A) The number of white blood cells in the peripheral blood of *Arid5b*^{OE} mice (solid bars, n=10) and wild-type litter mates (open bars, n=8). (B) The number of lymphocytes in the peripheral blood of *Arid5b*^{OE} mice (solid bars, n=10) and wild-type littermates (open bars, n=8). (C) The number of red blood cells in the peripheral blood of *Arid5b*^{OE} mice (solid bars, n=10) and wild-type littermates (open bars, n=8). (D) The number of B cells (B220^{+}), myeloid cells (Gr1^{+}/Mac1^{+}) and T cells (CD3^{+}) in the peripheral blood of *Arid5b*^{OE} mice (solid bars, n=9) and wild-type littermates (open bars, n=21). *P* values were estimated by a two-tail *t* test. **P*<0.05, ***P*<0.01, ****P*<0.001, *****P*<0.0001.

Supplementary Figure S1A), in which *Arid5b* upregulation can be induced with tetracycline and driven by the *Vav1* promoter. Assessed at the transcript level, *Arid5b* was upregulated 3-fold in bone marrow cells, 2-fold in the spleen, 3-fold in B220^{+} B cells, 2-fold in Mac1^{+}/Gr1^{+} myeloid cells, and 4-fold in Ter119^{+} erythroid cells, when compared to the same populations sorted from wild-type littermates (*Online Supplementary Figure S1B*). Gross examination of *Arid5b*^{OE} mice revealed no anatomical abnormalities. At 6-8 weeks of age, *Arid5b*^{OE} mice had a decrease in bone marrow cellularity compared to wild-type mice, although this was not observed in the spleen (*Online Supplementary Figure S5*). Phenotypic characterization of their peripheral blood revealed a significant reduction in the number of circulating white blood cells (Figure 1A), primarily driven by a lower lymphocyte count in *Arid5b*^{OE} mice (Figure 1B), with a modest reduction in the number of red blood cells (Figure 1C). There was also a significant decrease in the frequency of circulating B220^{+} cells, an increase in Mac1^{+} and Gr1^{+} cells, but no difference in CD3^{+} T cells in blood (Figure 1D). Both the frequency and the absolute number of B cells (mature and immature) were lower in both bone marrow (Figure 2A, *Online Supplementary Figure S6A*) and spleen (Figure 2B, *Online Supplementary Figure S6E*) of *Arid5b*^{OE} mice when compared to wild-type littermates, whereas *Arid5B* overexpression had little effect on CD4^{+} and CD8^{+} T-cell homeostasis (Figure 2C, D; *Online Supplementary Figure S6B, S6F*). In line with this, immunohistochemistry staining demonstrated many fewer B220^{+} B cells in the bone marrow (Figure 3A) and spleen (Figure 3C) of *Arid5b*^{OE} mice compared to wild-type littermates, but without obvious difference of CD3^{+} T cells in either bone marrow (Figure 3B) or spleen (Figure 3D).

By contrast, there was a slight increase in the frequency of myeloid cells in the bone marrow (Figure 4A) and spleen (Figure 4B) of *Arid5b*^{OE} mice compared to the frequency in their wild-type littermates, although the absolute cell numbers were similar between mice of these two genotypes (*Online Supplementary Figure S6C, G*). In addition, we observed an increase in erythroblast progenitor frequency and absolute number in the spleens of *Arid5b*^{OE} mice compared to wild-type littermates (Figure 4D; *Online Supplementary Figure S6H*), although this was not statistically significant in the bone marrow (Figure 4C; *Online Supplementary Figure S6D*). Analyzing hematopoietic stem and progenitor populations in the bone marrow, we noted a significant increase in the frequency and quantity of myeloid-biased multipotent progenitor 2 (MPP2) cells (*Online Supplementary Figure S7A, B*), with no difference observed in hematopoietic stem cells (HSC), MPP3, or MPP4

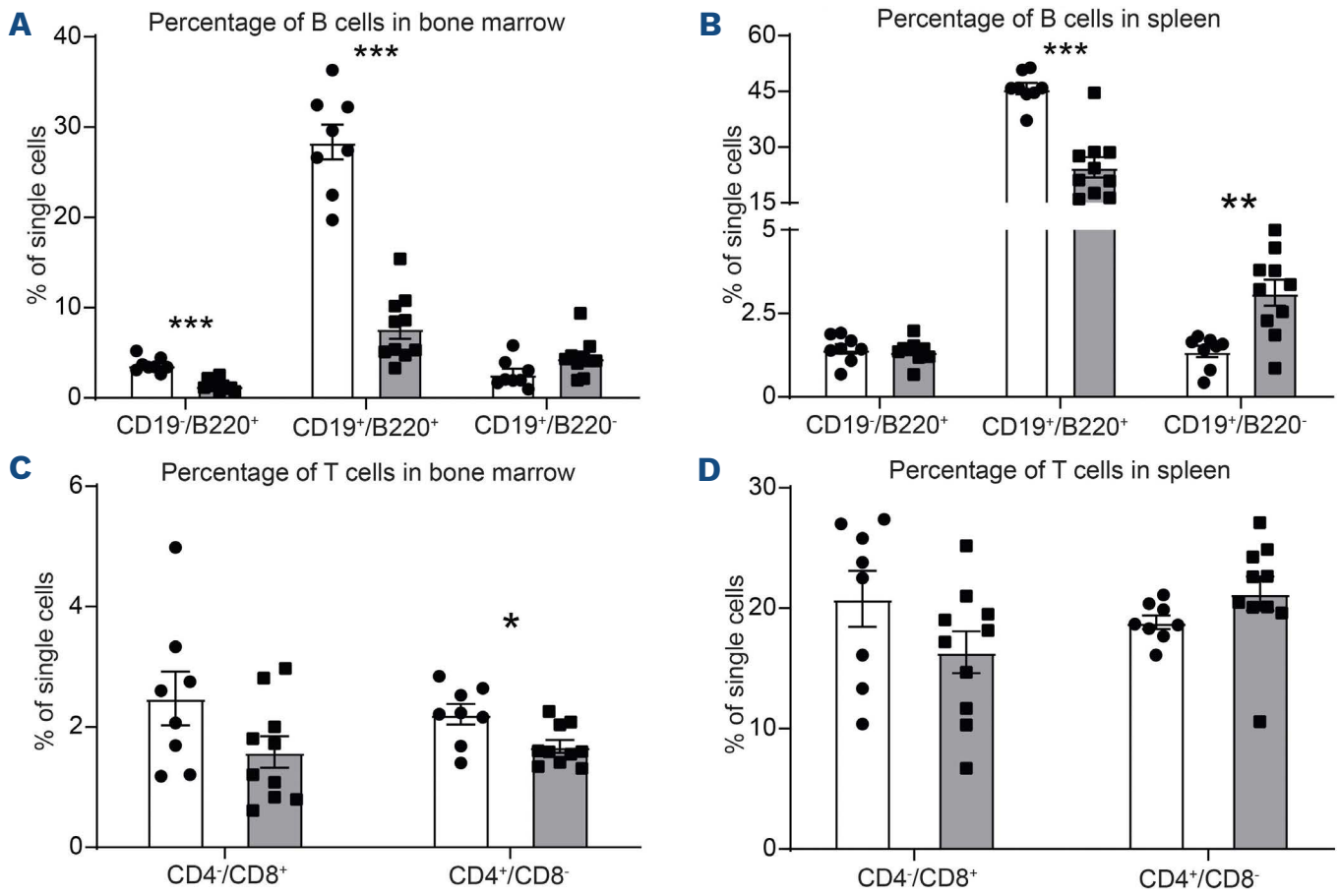

Figure 2. *Arid5b* overexpression results in the reduction of B cells in the bone marrow and spleen. (A, B) Percentage of B220$^+$ and CD19$^+$ B cells in the bone marrow and spleen of *Arid5b*^{OE} mice (solid bars, n=10) and wild-type littermates (open bars, n=8). (C, D) Percentage of CD4$^+$ and CD8$^+$ T cells in the bone marrow and spleen of *Arid5b*^{OE} mice (solid bars, n=10) and wild-type littermates (open bars, n=8). *P* values were estimated by a two-tail *t* test. **P*<0.05, ***P*<0.01, ****P*<0.001.

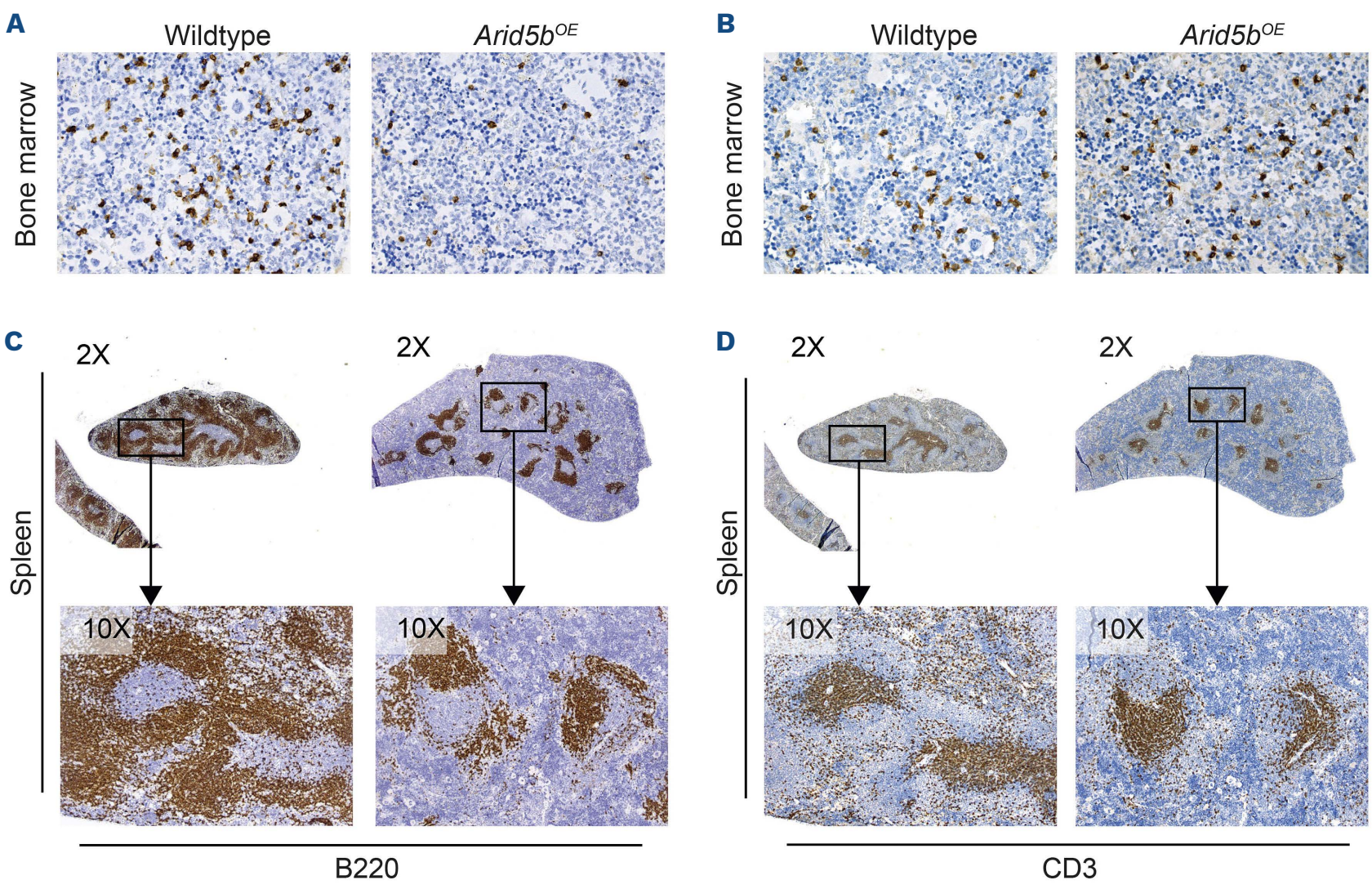

Figure 3. Representative immunohistochemistry staining of B cells in the bone marrow and spleen of *Arid5b*^{OE} *versus* wild-type mice. (A, C) Representative immunohistochemistry staining of B220$^+$ B cells in bone marrow and spleen from an *Arid5b*^{OE} mouse and wild-type littermate. (B, D) Representative immunohistochemistry staining of CD3$^+$ T cells in bone marrow and spleen from an *Arid5b*^{OE} mouse and wild-type littermate.

populations between *Arid5b* genotypes. An enhanced myeloid colony-forming ability of bone marrow cells from *Arid5b*^{OE} mice was observed when compared to that of wild-type littermates, mainly driven by increased granulocyte and/or macrophage progenitor cells (granulocytes, macrophages, granulocyte-macrophage) and multi-potential progenitor cells (*Online Supplementary Figure S7C*).

Arid5b regulates B-cell development in bone marrow

B-cell lymphopoiesis from hematopoietic progenitors occurs in sequential stages in the bone marrow. To determine which stages were affected in *Arid5b*^{OE} mice, B cells were analyzed using flow cytometry according to the Hardy fraction scheme.[32] Quantification of the proportion and number of pre-pro-B cells (Fraction A), pro-B cells (Fraction B), small pre-B cells (Fraction D), immature B cells (Fraction E) and mature B cells (Fraction F) revealed a significant reduction in the frequency and quantity of these populations in the bone marrow of *Arid5b*^{OE} mice compared to their wild-type littermates (Figure 5A, B). Interestingly, we found significant increases in apoptosis in both Fractions B and C in *Arid5b*^{OE} mice (Figure 5C), but no change in the cycling profile of other B cells (*Online Supplementary Figure S8*). Testing the differentiation capacity of B-cell progenitors *in vitro*, we found that *Arid5b*^{OE} bone marrow cells produced significantly fewer pre-B-cell colonies when compared to wild-type littermates in the presence of IL-7 (Figure 5D).

Effects of *Arid5b* deficiency on normal hematopoiesis were also analyzed in *Mb1*- and *Vav1*-driven *Arid5b* knockout mouse models (*Arid5b*^{KO}) (*Online Supplementary Figure S9*). In contrast to the overexpression mouse model, the proportion of the pre-B-cell population (Fraction D) was significantly increased in the bone marrow of both *Mb1*-driven and *Vav1*-driven *Arid5b*^{KO} mice compared to their wild-type littermates (*Online Supplementary Figure S10A, D*). By contrast, no significant changes were noted in hematopoietic stem cells (HSC^{LT} and HSCST), or progenitor cell populations (MPP2, MPP3, and MPP4), and myeloid cells in the bone marrow, spleen, and peripheral blood (*Online Supplementary Figures S10B, C, E, F* and *S11*).

Arid5b regulates B-cell development in secondary lymphoid organs

We extended our analysis of B lymphopoiesis to the spleen and peritoneal cavity. B-cell populations in the spleen were divided into four subsets: transitional type 1 B (T1) cells, transitional type 2 B (T2) cells, marginal zone B (MZ) cells, and follicular B (FO) cells. While the transitional and MZ B-cell subsets appeared to be unaffected by the overexpression of *Arid5b*, we found a significant reduction in the proportion and total number of follicular B cells relative to those in wild-type mice (Figure 6A, B). In the peritoneal cavity B cells, there was also a significant re-

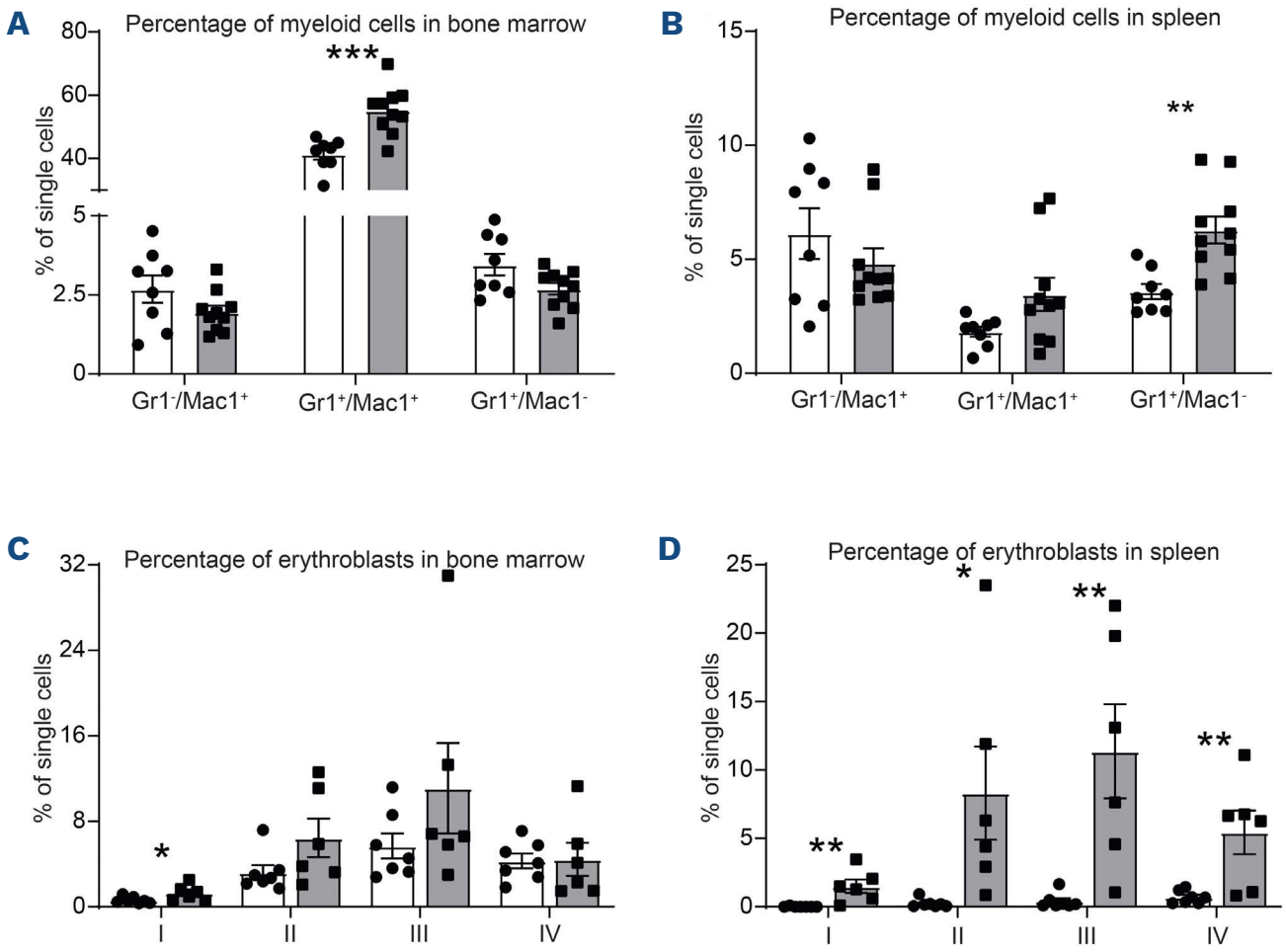

Figure 4. *Arid5b* overexpression alters the development of myeloid and erythroid cells in the bone marrow and spleen. (A, B) Total Gr1$^+$ and Mac1$^+$ myeloid cells in the bone marrow and spleen of *Arid5b*^{OE} mice (solid bars, n=10) and wild-type littermates (open bars, n=8). (C, D) Total Ter119$^+$ and CD71$^+$ erythroblasts in the bone marrow and spleen of *Arid5b*^{OE} mice (solid bars, n=6) and wild-type littermates (open bars, n=7). *P* values were estimated by a two-tail *t* test. **P*<0.05, ***P*<0.01, ****P*<0.001.

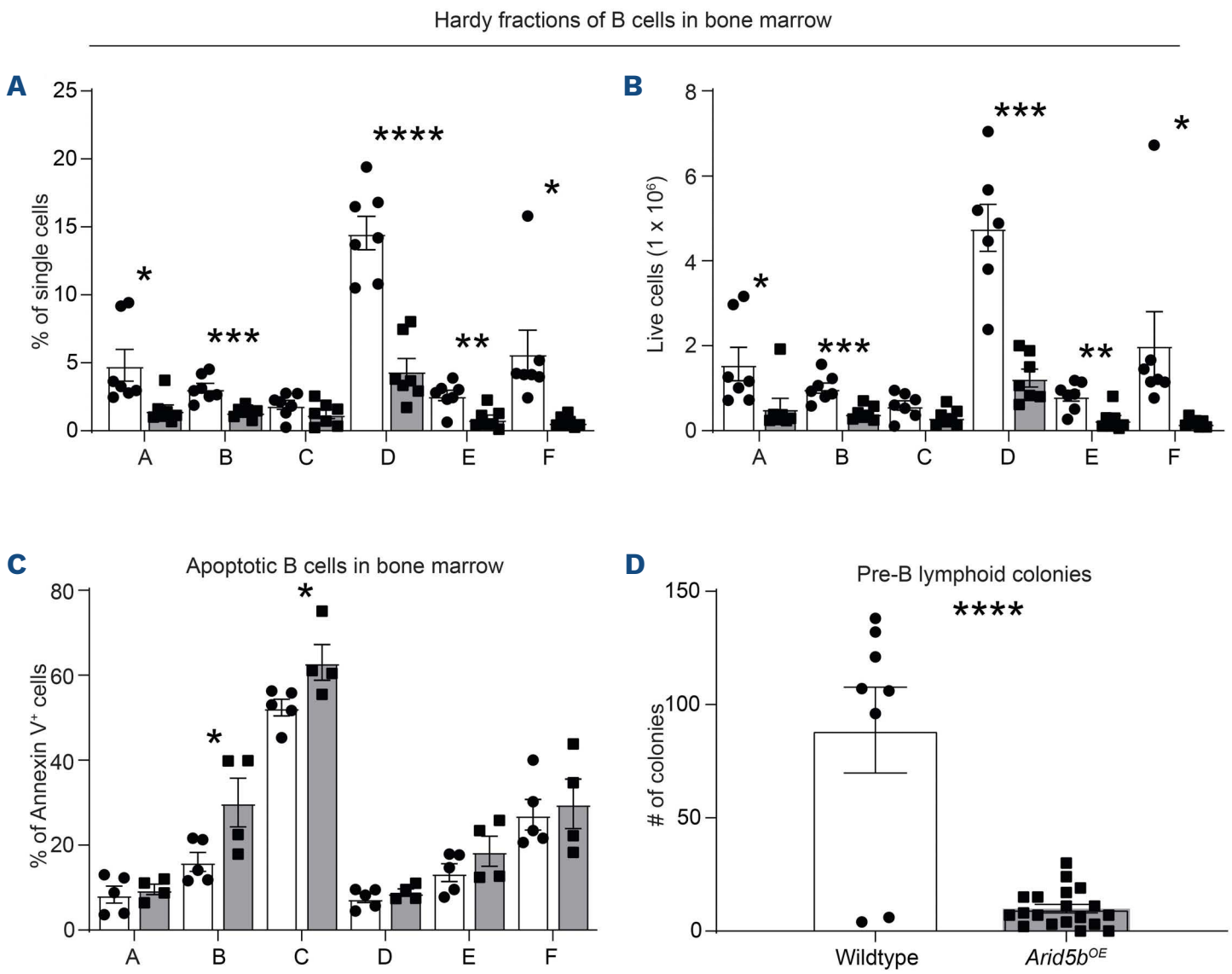

Figure 5. B-cell development in the bone marrow of *Arid5b*^{OE} *versus* wild-type mice. (A, B) Frequency and the absolute number of B-cell subsets in the bone marrow of *Arid5b*^{OE} mice (solid bars, n=7) and wild-type littermates (open bars, n=7). (C) Percentage of annexin V^{+} cells in various bone marrow B-cell subsets of *Arid5b*^{OE} mice (solid bars, n=4) and wild-type littermates (open bars, n=5). (D) Pre-B colony-forming units per 200,000 bone marrow cells from *Arid5b*^{OE} (solid bars, n=19) or wild-type littermates (open bars, n=8): experiment performed in replicate, using MethoCult M3630. *P* values were estimated by a two-tail *t* test. **P*<0.05, ***P*<0.01, ****P*<0.001, *****P*<0.0001.

duction in both B1a and B1b subsets in *Arid5b*^{OE} mice (Figure 6C, D), but no difference in B2 B cells.

Arid5b influences B-cell activity and metabolism

To assess the role of *Arid5b* in B-cell activation, we purified CD43^{-} resting splenic B cells to be stimulated with anti-IgM and IL-4 or LPS. We found that LPS induced proliferation in both wild-type and *Arid5b*^{OE} B cells. Surprisingly, anti-IgM- and IL-4-induced proliferation was much less significant in B cells from *Arid5b*^{OE} mice (Figure 7A), and these cells were also significantly more apoptotic 48 hours after stimulation (Figure 7B). Furthermore, the proliferation defect was consistent across a wide range of anti-IgM antibody concentrations (Figure 7C). Spleen B cells from *Arid5b*^{OE} mice exhibited a significantly lower level of surface IgD, suggesting a partial maturation blockade at the IgD-negative stage (Figure 7D). In the presence of anti-IgM and IL-4, CD69 and CD86 were both upregulated but to a much lesser degree in *Arid5b*^{OE} B cells than in B cells from wild-type littermates, 24 hours after stimulation (Figure 7E).

To further explore this, we examined B-cell receptor signaling in B cells with or without *Arid5b* overexpression using the same activation model mentioned above. Compared to cells from wild-type mice, *Arid5b*^{OE} cells exhibited higher levels of pBTK and pSYK at baseline and these rose upon anti-IgM and IL-4 stimulation (Figure 8A, B). However, the degree of increase of these two phospho-proteins was significantly smaller with *Arid5b*^{OE}, suggesting attenuated activation. Similarly, pAKT level was also higher at baseline in *Arid5b*^{OE} cells with less activation by anti-IgM and IL-4 stimulation compared to that in wild-type cells (Figure 8C). Interestingly, there were also significantly higher levels of surface expression of VpreB and λ5 on CD19^{+} B cells from *Arid5b*^{OE} mice than from wild-type mice (Figure 8D). Studies have shown that B cells undergo metabolic changes upon activation.[33,34] These changes include increases in oxygen consumption rate (OCR) which is an indicator of oxidative phosphorylation. Our data suggest that at steady-state the B cells from *Arid5b*^{OE} mice are more active than their wild-type B-cell counterparts. We found that naïve B cells isolated from *Arid5b*^{OE} mice had in-

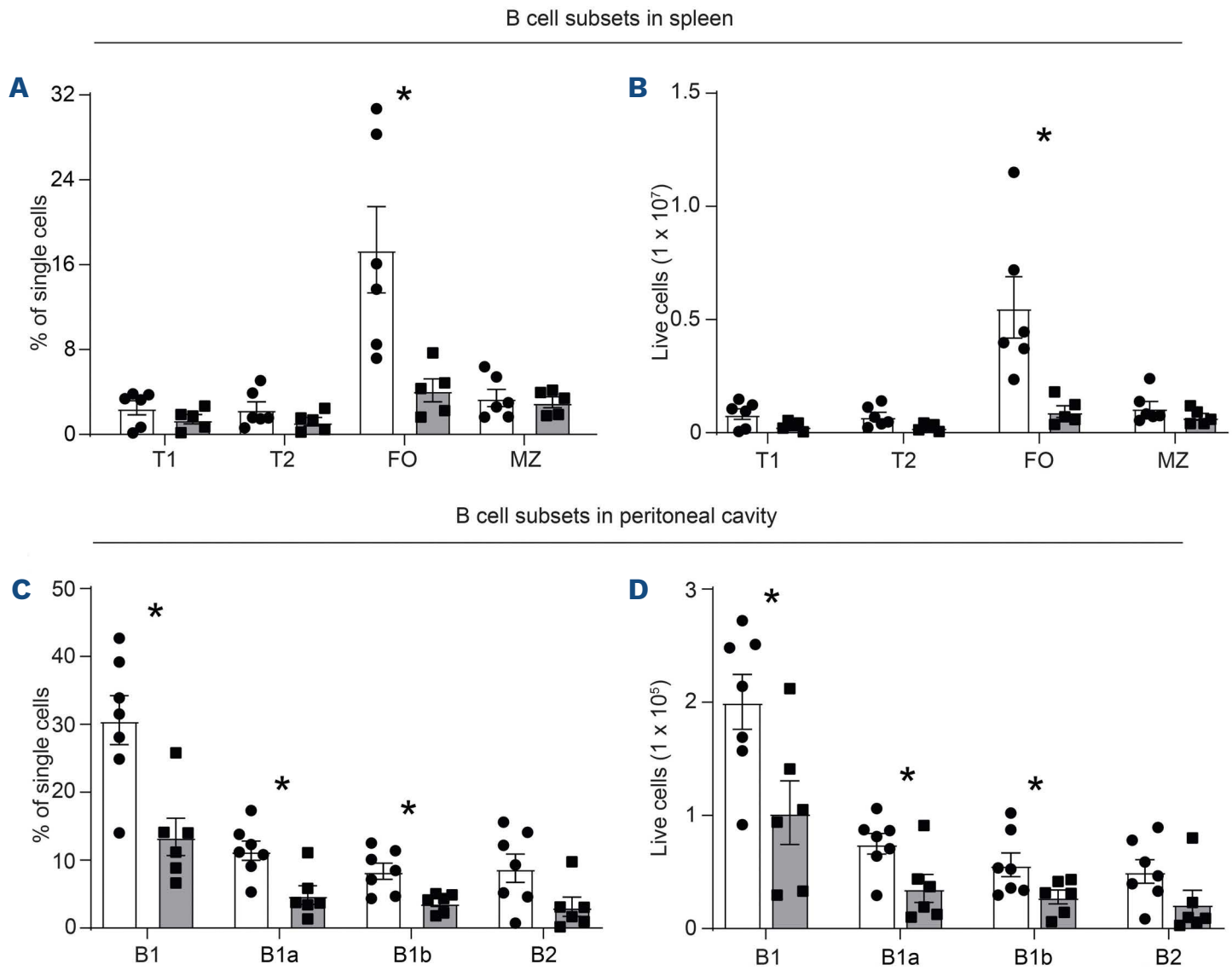

Figure 6. *Arid5b* overexpression disrupts B-cell development in the spleen and peritoneal cavity. (A, B) Frequency and absolute number of spleen B cells in *Arid5b*^{OE} mice (solid bars, n=5) and wild-type littermates (open bars, n=6). (C, D) Frequency of B-cell subsets in the peritoneal cavity of *Arid5b*^{OE} mice (solid bars, n=6) and wild-type littermates (open bars, n=7). *P* values were estimated by a two-tail *t* test. **P*<0.05, ***P*<0.01, ****P*<0.001, *****P*<0.0001.

creased OCR when compared to naïve B cells from wild-type littermates (*Online Supplementary Figure S12A*). Next, we wanted to gain more insight into the metabolism of B cells from *Arid5b*^{OE} mice after stimulation with either LPS or anti-IgM and IL-4. We measured the OCR and found that the baseline OCR of *Arid5b*^{OE} stimulated B cells was higher than that of wild-type mice and showed greater maximum mitochondrial respiration capacity (*Online Supplementary Figure S12B*). These results together suggested hyperactivation of B cells from *Arid5b*^{OE} mice compared to their wild-type B-cell counterparts.

Discussion

The genomic region encompassing the *ARID5B* gene on 10q21.2 is one of the strongest genome-wide association study hits with robust association with ALL risk replicated consistently.[9,10,13,35,36] Despite the overwhelming evidence for genetic association with this cancer, the molecular mechanisms by which *ARID5B* influences normal hematopoiesis have remained poorly understood. Therefore, our study addressed this knowledge gap by developing mouse models to directly determine hematopoietic consequences of *ARID5B* deregulation *in vivo*. Our results showed that overexpression of *Arid5b* in the mouse hematopoietic system results in marked disruption of B-cell development *in vivo*; B cells with *Arid5B* overexpression also exhibited defective activation *in vitro* in response to stimuli with abnormal mitochondria respiration.

Early studies of *Arid5b* null mice showed significant alteration in lymphoid development although systematic hematopoietic phenotyping was not performed,[25] and these results were confounded by the mixed genetic background of these animals.[26] In our model systems, *Arid5b* overexpression resulted in remarkable loss of B cells across different developmental stages. Even B cells that reached the terminally differentiated stage failed to be activated by anti-IgM and IL4 stimulation. These cells exhibited a higher propensity for apoptosis and attenuated expression of CD69 and CD86. They were characterized by hyperactive BTK and SYK at baseline compared to B cells from wild-type mice, and were then unresponsive to stimuli *in vitro*. The effects of *ARID5B* on B-cell de-

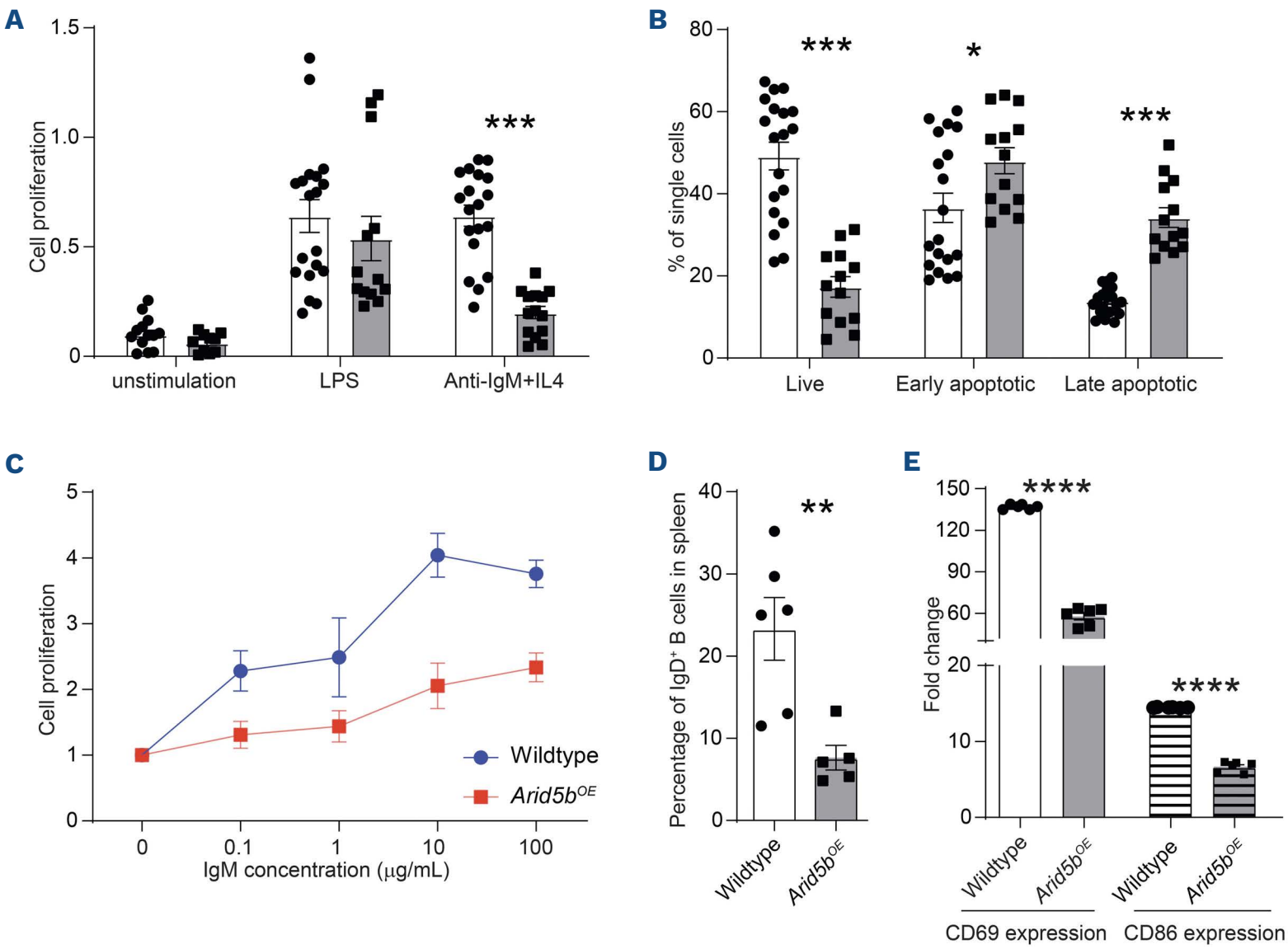

Figure 7. *Arid5b* overexpression results in defective B-cell activation. (A) Absolute absorbance value from an MTS proliferation assay in three groups of B cells maintained in RPMI 1640 for 48 hours: unstimulated, stimulated with lipopolysaccharide (LPS), and stimulated with IgM F(ab')$_2$ fragment and interleukin-4 (IL-4). Wild-type mice are represented by open bars (n=19) and *Arid5b*^{OE} mice by solid bars (n=13). (B) B-cell apoptosis was evaluated 48 hours after treatment with IgM F(ab')$_2$ fragment and IL-4 using annexin V and 7-amino actinomycin D in wild-type (open bars, n=19) and *Arid5b*^{OE} cells (solid bars, n=13). (C) The MTS assay was performed 24 hours after treatment of B cells from wild-type and *Arid5b*^{OE} mice with varying concentrations of IgM F(ab')$_2$ fragment. Absorbance was normalized to that of unstimulated cells. (D) Frequency of IgD-expressing B cells in the spleen of *Arid5b*^{OE} mice (solid bars, n=6) and wild-type littermates (open bars, n=5). (E) Fold change in cell surface expression of the activation markers CD69 and CD86 on B cells 24 hours after treatment with IgM F(ab')$_2$ fragment and IL-4. Expression was normalized to that of unstimulated cells. Wild-type mice are represented by open bars (n=6) and *Arid5b*^{OE} mice by solid bars (n=6). *P* values were estimated by a two-tail *t* test. **P*<0.05, ***P*<0.01, ****P*<0.001, *****P*<0.0001.

velopment and function are of relevance not only because ALL primarily arises in B progenitor cells, but more importantly *ARID5B* has also been implicated by genome-wide association studies in a range of autoimmune diseases such as rheumatoid arthritis and systemic lupus erythematosus.[37,38] Particularly in lupus, aberrant B-cell activation and the production of pathogenic autoantibodies are hallmarks of this disease.[39] The ALL risk allele at the *ARID5B* single nucleotide polymorphism was associated with lower transcription *in-cis*,[40] linking *ARID5B* downregulation to leukemogenesis. Taken together, these results point to *ARID5B* as an important regulator of lymphoid development, especially in the B-cell lineage.

In addition, we also explored the effects of *Arid5b* loss using both *Mb1*-driven and *Vav1*-driven knockout mouse models. Compared to wild-type littermates, these mice exhibited modest (but significant) increases of Hardy Fractions C and D within the B-cell compartment in the bone marrow of *Mb1*-driven *Arid5b*^{KO} mice (*Online Supplementary Figure S10A*) or Hardy Fractions D and E in *Vav1*-driven *Arid5b*^{KO} mice (*Online Supplementary Figure S10D*). However, we cannot definitively conclude whether the observed effects of *Arid5b* overexpression or knockout are completely cell autonomous, especially in the *Vav1*-driven models in which cells of multiple lineages can influence each other. Interestingly, our data suggest that *Arid5b* overexpression alters glucose metabolism with enhanced oxidative phosphorylation. Thus, one could speculate that the loss of *ARID5B* would result in decreased oxidative phosphorylation, which has been documented in B-ALL.[41]

It should be noted that none of our *Arid5b* mouse models developed overt B-ALL and therefore the direct link of *ARID5B* with leukemogenesis remains to be established.

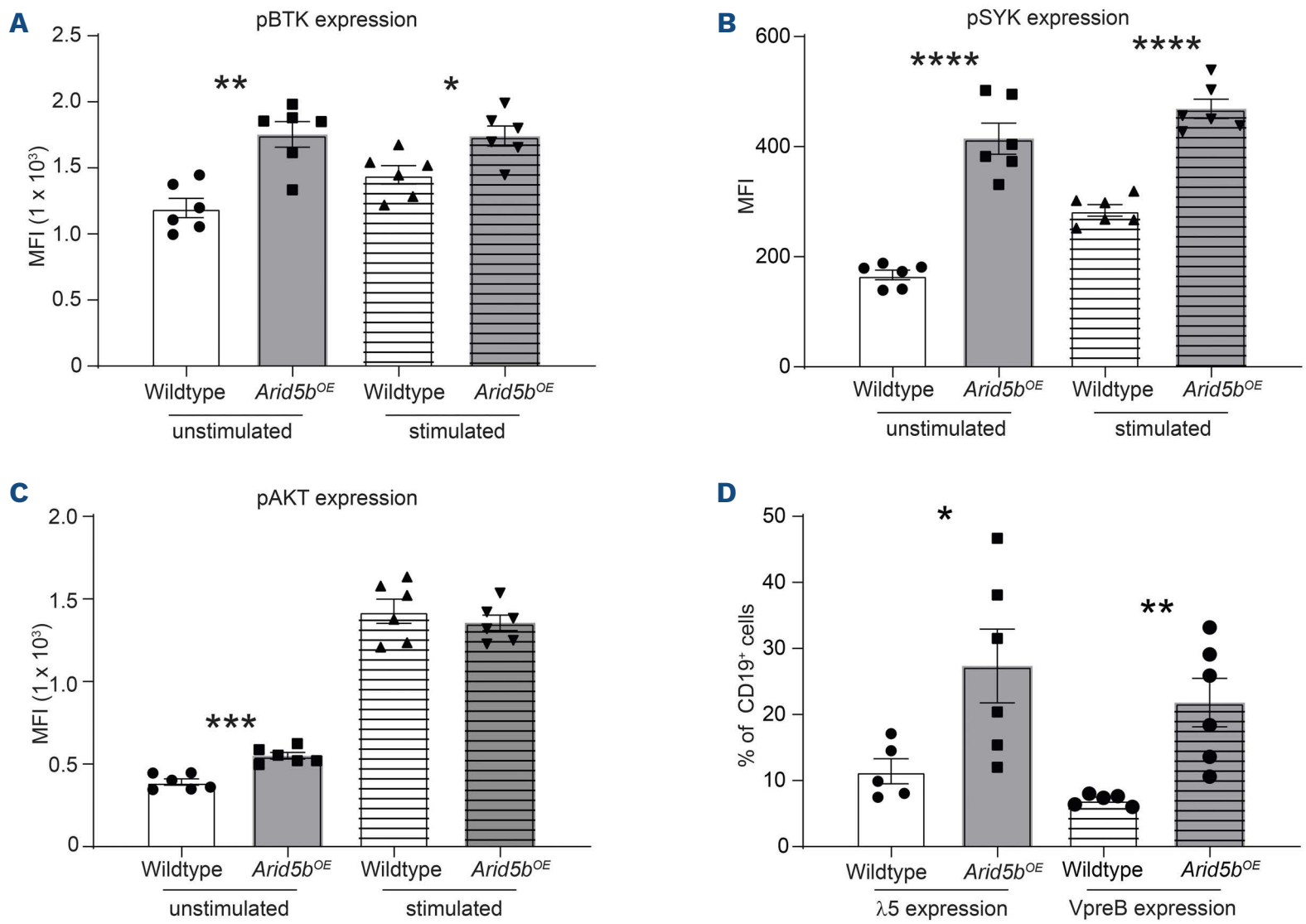

Figure 8. *Arid5b* overexpression and defects in B-cell receptor signaling of B cells. (A, B) Mean fluorescence intensity (MFI) for pBTK and pSYK levels in B cells 24 hours after treatment with IgM F(ab')$_2$ fragment and interleukin-4 (IL-4). Wild-type mice are represented by open bars (n=6) and *Arid5b*^{OE} mice by solid bars (n=6). (C) MFI for pAKT levels in B cells 24 hours after treatment with IgM F(ab')$_2$ fragment and IL-4. Wild-type mice are represented by open bars (n=6) and *Arid5b*^{OE} mice by solid bars (n=6). (D) Surface expression of λ5 and VpreB on CD19$^+$ B cells of *Arid5b*^{OE} mice (solid bars, n=6) and wild-type littermates (open bars, n=6). *P* values were estimated by a two-tail *t* test. **P*<0.05, ***P*<0.01, ****P*<0.001, *****P*<0.0001.

It is plausible that *Arid5b* deregulation alone is insufficient to induce leukemia without co-operating mutations in other oncogenes or tumor suppressors, with only modest effects on leukemia development *in vivo*. Or *ARID5B* could only influence leukemogenesis when expressed at a precise level that is probably not recapitulated by ectopic overexpression or knockout in our models. Interestingly, *Arid5b*^{OE} mice also survived for a shorter time compared to wild-type controls, with signs of hemolytic anemia (*data not shown)*, and future studies are warranted to investigate these phenotypes. Nevertheless, alterations in B-cell differentiation and function in *Arid5b*^{OE} and *Arid5b*^{KO} mice pointed to the role of this gene in lineage development and relevance to B-ALL. Our comprehensive hematopoietic phenotyping also helped paint a broad picture of *ARID5B* function, although the detailed molecular mechanisms remain incomplete.

In conclusion, we mechanistically explored the role of *ARID5B* in hematopoiesis. Our results provided novel insights into the biological functions of ARID5B in normal hematopoiesis, especially B-cell lymphopoiesis, further implicating this gene in B-cell-related diseases broadly.

Disclosures

JJY receives research funding from Takeda Pharmaceutical company. The other authors have no potential conflicts of interest to disclose.

Contributions

JJY is the principal investigator of this study, has full access to all the data in the study, and takes responsibility for the integrity of the data and the accuracy of the data analysis. CG and XZ performed the experiments and analyzed the data. JJY, CG, and XZ wrote the manuscript. SMF and HZ contributed reagents, materials and/or data. JJY, XZ, CG, interpreted the data and the research findings. All the co-authors reviewed the manuscript.

Acknowledgments

We thank the patients and parents who participated in the clinical trials included in this study. We thank Dr. Omar I

Abdel-Wahab for his advice on Arid5b mouse studies. We thank Keith A. Laycock, PhD, ELS, for scientific editing of the article.

Funding

This work was supported by the National Institutes of Health (CA176063), and by the American Lebanese Syrian Associated Charities (ALSAC). The content is solely the responsibility of the authors and does not necessarily represent the official views of the U.S. National Institutes of Health.

Data-sharing statement

All data needed to evaluate the conclusions in the paper are present in the paper and/or the Online Supplementary Materials.

References

1. Pui CH, Robison LL, Look AT. Acute lymphoblastic leukaemia. Lancet. 2008;371(9617):1030-1043.
2. Hunger SP, Mullighan CG. Acute lymphoblastic leukemia in children. N Engl J Med. 2015;373(16):1541-1552.
3. Moriyama T, Relling MV, Yang JJ. Inherited genetic variation in childhood acute lymphoblastic leukemia. Blood. 2015;125(26):3988-3995.
4. Garber JE, Goldstein AM, Kantor AF, Dreyfus MG, Fraumeni JF Jr, Li FP. Follow-up study of twenty-four families with Li-Fraumeni syndrome. Cancer Res. 1991;51(22):6094-6097.
5. Hemminki K, Jiang Y. Risks among siblings and twins for childhood acute lymphoid leukaemia: results from the Swedish Family-Cancer Database. Leukemia. 2002;16(2):297-298.
6. Greaves MF, Maia AT, Wiemels JL, Ford AM. Leukemia in twins: lessons in natural history. Blood. 2003;102(7):2321-2333.
7. Trevino LR, Yang W, French D, et al. Germline genomic variants associated with childhood acute lymphoblastic leukemia. Nat Genet. 2009;41(9):1001-1005.
8. Papaemmanuil E, Hosking FJ, Vijayakrishnan J, et al. Loci on 7p12.2, 10q21.2 and 14q11.2 are associated with risk of childhood acute lymphoblastic leukemia. Nat Genet. 2009;41(9):1006-1010.
9. Yang W, Trevino LR, Yang JJ, et al. ARID5B SNP rs10821936 is associated with risk of childhood acute lymphoblastic leukemia in blacks and contributes to racial differences in leukemia incidence. Leukemia. 2010;24(4):894-896.
10. Yang JJ, Xu H, Yang WJ, et al. Genome-wide association study identifies a novel susceptibility locus at 10p12.31-12.2 for childhood acute lymphoblastic leukemia in ethinically diverse populations. Blood. 2012;120(21):877.
11. Perez-Andreu V, Roberts KG, Harvey RC, et al. Inherited GATA3 variants are associated with Ph-like childhood acute lymphoblastic leukemia and risk of relapse. Nat Genet. 2013;45(12):1494-1498.
12. Xu H, Cheng C, Devidas M, et al. ARID5B genetic polymorphisms contribute to racial disparities in the incidence and treatment outcome of childhood acute lymphoblastic leukemia. J Clin Oncol. 2012;30(7):751-757.
13. Xu H, Yang WJ, Perez-Andreu V, et al. Novel susceptibility variants at 10p12.31-12.2 for childhood acute lymphoblastic leukemia in ethnically diverse populations. J Natl Cancer Inst. 2013;105(10):733-742.
14. Vijayakrishnan J, Kumar R, Henrion MY, et al. A genome-wide association study identifies risk loci for childhood acute lymphoblastic leukemia at 10q26.13 and 12q23.1. Leukemia. 2017;31(3):573-579.
15. Prasad RB, Hosking FJ, Vijayakrishnan J, et al. Verification of the susceptibility loci on 7p12.2, 10q21.2, and 14q11.2 in precursor B-cell acute lymphoblastic leukemia of childhood. Blood. 2010;115(9):1765-1767.
16. Healy J, Richer C, Bourgey M, Kritikou EA, Sinnett D. Replication analysis confirms the association of ARID5B with childhood B-cell acute lymphoblastic leukemia. Haematologica. 2010;95(9):1608-1611.
17. Evans TJ, Milne E, Anderson D, et al. Confirmation of childhood acute lymphoblastic leukemia variants, ARID5B and IKZF1, and interaction with parental environmental exposures. PloS One. 2014;9(10):e110255.
18. Migliorini G, Fiege B, Hosking FJ, et al. Variation at 10p12.2 and 10p14 influences risk of childhood B-cell acute lymphoblastic leukemia and phenotype. Blood. 2013;122(19):3298-3307.
19. Walsh KM, de Smith AJ, Chokkalingam AP, et al. Novel childhood ALL susceptibility locus BMI1-PIP4K2A is specifically associated with the hyperdiploid subtype. Blood. 2013;121(23):4808-4809.
20. Studd JB, Vijayakrishnan J, Yang M, Migliorini G, Paulsson K, Houlston RS. Genetic and regulatory mechanism of susceptibility to high-hyperdiploid acute lymphoblastic leukaemia at 10p21.2. Nat Commun. 2017;8:14616.
21. Whitson RH, Huang T, Itakura K. The novel Mrf-2 DNA-binding domain recognizes a five-base core sequence through major and minor-groove contacts. Biochem Biophys Res Commun. 1999;258(2):326-331.
22. Yuan YC, Whitson RH, Itakura K, Chen Y. Resonance assignments of the Mrf-2 DNA-binding domain. J Biomol NMR. 1998;11(4):459-460.
23. Yuan YC, Whitson RH, Liu Q, Itakura K, Chen Y. A novel DNA-binding motif shares structural homology to DNA replication and repair nucleases and polymerases. Nat Struct Biol. 1998;5(11):959-964.
24. Zhu L, Hu J, Lin D, Whitson R, Itakura K, Chen Y. Dynamics of the Mrf-2 DNA-binding domain free and in complex with DNA. Biochemistry. 2001;40(31):9142-9150.
25. Lahoud MH, Ristevski S, Venter DJ, et al. Gene targeting of Desrt, a novel ARID class DNA-binding protein, causes growth retardation and abnormal development of reproductive organs. Genome Res. 2001;11(8):1327-1334.
26. Whitson RH, Tsark W, Huang TH, Itakura K. Neonatal mortality and leanness in mice lacking the ARID transcription factor Mrf-2. Biochem Biophys Res Commun. 2003;312(4):997-1004.
27. Watanabe M, Layne MD, Hsieh CM, et al. Regulation of smooth muscle cell differentiation by AT-rich interaction domain transcription factors Mrf2alpha and Mrf2beta. Circ Res. 2002;91(5):382-389.
28. Baba A, Ohtake F, Okuno Y, et al. PKA-dependent regulation of the histone lysine demethylase complex PHF2-ARID5B. Nat Cell Biol. 2011;13(6):668-675.
29. Cichocki F, Wu CY, Zhang B, et al. ARID5B regulates metabolic programming in human adaptive NK cells. J Exp Med. 2018;215(9):2379-2395.

30. Leong WZ, Tan SH, Ngoc PCT, et al. ARID5B as a critical downstream target of the TAL1 complex that activates the oncogenic transcriptional program and promotes T-cell leukemogenesis. Genes Dev. 2017;31(23-24):2343-2360.
31. Guo B, Rothstein TL. IL-4 upregulates Igalpha and Igbeta protein, resulting in augmented IgM maturation and B cell receptor-triggered B cell activation. J Immunol. 2013;191(2):670-677.
32. Hardy RR, Carmack CE, Shinton SA, Kemp JD, Hayakawa K. Resolution and characterization of pro-B and pre-pro-B cell stages in normal mouse bone marrow. J Exp Med. 1991;173(5):1213-1225.
33. Akkaya M, Traba J, Roesler AS, et al. Second signals rescue B cells from activation-induced mitochondrial dysfunction and death. Nat Immunol. 2018;19(8):871-884.
34. Waters LR, Ahsan FM, Wolf DM, Shirihai O, Teitell MA. Initial B cell activation induces metabolic reprogramming and mitochondrial remodeling. iScience. 2018;5:99-109.
35. Vijayakrishnan J, Qian M, Studd JB, et al. Identification of four novel associations for B-cell acute lymphoblastic leukaemia risk. Nat Commun. 2019;10(1):5348.
36. Xu H, Cheng C, Devidas M, et al. ARID5B genetic polymorphisms contribute to racial disparities in the incidence and treatment outcome of childhood acute lymphoblastic leukemia. J Clin Oncol. 2012;30(7):751-757.
37. Okada Y, Terao C, Ikari K, et al. Meta-analysis identifies nine new loci associated with rheumatoid arthritis in the Japanese population. Nat Genet. 2012;44(5):511-516.
38. Tomer Y, Hasham A, Davies TF, et al. Fine mapping of loci linked to autoimmune thyroid disease identifies novel susceptibility genes. J Clin Endocrinol Metab. 2013;98(1):E144-152.
39. Kil LP, Hendriks RW. Aberrant B cell selection and activation in systemic lupus erythematosus. Int Rev Immunol. 2013;32(4):445-470.
40. Zhao X, Qian M, Goodings C, et al. Molecular mechanisms of ARID5B-mediated genetic susceptibility to acute lymphoblastic leukemia. J Natl Cancer Inst. 2022;114(9):1287-1295.
41. Boag JM, Beesley AH, Firth MJ, et al. Altered glucose metabolism in childhood pre-B acute lymphoblastic leukaemia. Leukemia. 2006;20(10):1731-1737.